Nanoscale

MINIREVIEW

View Article Online
View Journal | View Issue

Cite this: *Nanoscale*, 2023, **15**, 18173

An emerging direction for nanozyme design: from single-atom to dual-atomic-site catalysts

Ying Wang,[a] Yong Wang,[a] Lawrence Yoon Suk Lee *[a,b] and Kwok-Yin Wong *[a]

Nanozymes, a new class of functional nanomaterials with enzyme-like characteristics, have recently made great achievements and have become potential substitutes for natural enzymes. In particular, single-atomic nanozymes (Sazymes) have received intense research focus on account of their versatile enzyme-like performances and well-defined spatial configurations of single-atomic sites. More recently, dual-atomic-site catalysts (DACs) containing two neighboring single-atomic sites have been explored as next-generation nanozymes, thanks to the flexibility in tuning active sites by various combinations of two single-atomic sites. This minireview outlines the research progress of DACs in their synthetic approaches and the latest characterization techniques highlighting a series of representative examples of DAC-based nanozymes. In the final remarks, we provide current challenges and perspectives for developing DAC-based nanozymes as a guide for researchers who would be interested in this exciting field.

Received 26th September 2023,
Accepted 12th October 2023

DOI: 10.1039/d3nr04853e

rsc.li/nanoscale

1. Introduction

Nanozymes, a class of nanomaterials with intrinsic enzyme-like activities, are considered next-generation artificial enzymes.[1–3] Compared with natural enzymes, nanozymes offer the unique advantages of low cost, high stability, tunable catalytic activity, and easy recyclability, features that greatly promote the integration of traditional chemical catalysts and biocatalysts.[4,5] To date, various nanomaterials that show enzyme-like catalytic activities, including noble metals, transition metal oxides, and metal–organic frameworks (MOF), have been discovered.[6–9] They have shown great application prospects in biosensing detection,[10,11] biomedicine treatment,[5,12] food safety,[13] and environmental protection.[14] However, plenty of challenges remain in employing these nanozymes as enzyme alternatives. Firstly, the heterogeneous nanostructures of nanozymes inevitably yield inhomogeneous composition (size, exposed crystal plane, valence state, and defects), which leads to unsatisfactory enzyme-like selectivity, unclear catalytic active sites, and ambiguous reaction mechanisms.[15] Secondly, the synthetic methods of nanozymes make it rather difficult to fine-tune their structure, and the efficiency of metal utilization is usually insufficient, which leads to undesired or limited enzyme-like activities. To overcome these limitations, new design approaches for constructing nanozymes with controllable and homogeneous configurations are crucial.

With the rapid development of nanotechnology,[16] single-atom catalysts (SACs) have recently emerged and received great attention in the fields of electrocatalysis,[17] photocatalysis,[18] biocatalysis,[19,20] and thermo-catalysis.[21] SACs integrate the merits of homogeneous and heterogeneous catalysts with maximal atomic usage and unique site structures.[22,23] Multitudinous well-defined SACs have been successfully applied as bioinspired single-atom nanozymes (SAzymes).[24] For example, SAzymes containing Fe,[25,26] Co,[27] Ni,[28] Cu,[29] Zn,[30] Cr, Mn,[31] Mo,[32] Pt,[33] Ru, Rh, Ir, Pd,[34] and Au single-atomic sites anchored on a carbon base,[35] N, S, P, B, and F doped carbon-based SAzymes,[36] and SAzymes with metal oxide-based supports have been prepared and applied in the fields of biosensing,[10] biomedicine,[37] environmental treatment,[38] and food safety analysis.[13] The atomically precise configuration of SAzymes also provides ideal models to understand the structure–performance relationship and enzyme-like catalytic mechanisms.[39] Thus, the enzyme-like activity and specificity of SAzymes can be precisely adjusted and regulated at the atomic level, which makes them a promising candidate for next-generation nanozymes.[40] Despite the success of SAzymes so far, there are still some burning questions to be answered: (1) How can linear scaling relations between different intermediates in enzyme-like reactions be broken for the simple active site of SAzymes? (2) How can the enzyme-like activities of SAzymes be further improved when the loading

[a]*Department of Applied Biology and Chemical Technology and the State Key Laboratory of Chemical Biology and Drug Discovery, The Hong Kong Polytechnic University, Hung Hom, Kowloon, Hong Kong SAR, China.*
E-mail: lawrence.ys.lee@polyu.edu.hk, kwok-yin.wong@polyu.edu.hk
[b]*Research Institute for Smart Energy, The Hong Kong Polytechnic University, Hung Hom, Kowloon, Hong Kong SAR, China*

amount of a single atom is limited due to metal aggregation? The answers to these questions can be found by exploring advanced strategies for configuring new SAzymes.

In nature, the existence of unique cofactors, together with active centers, plays a synergistic role in the functioning of natural enzymes. For instance, cytochrome c oxidase (CcO) is mainly composed of binuclear sites consisting of a single Cu_B site and a heme a_3 site, which are a cofactor and an active center, respectively.[41] Also, carbon monoxide dehydrogenase and nitrogenase possess active centers configured with dual-metal atomic sites.[42] Inspired by these natural paradigms, dual-atomic catalysts (DACs) have been proposed as an extended and improved version of SACs. In addition to the advantages of atomically defined structures similar to those of SACs, DACs can offer more accessible active sites with the potential to break the linear relationship limitation in enzymatic reactions.[43] Since Warner *et al.* first reported the characteristics of Fe DACs embedded in graphene vacancies in 2014,[44] DACs have attracted extensive attention, particularly in the catalysis field, and a variety of DACs with unique features, such as adjacent homo-metal sites,[45] adjacent hetero-metal sites,[46] and separated hetero-metal sites, are engaged in heterogeneous catalysis reactions, demonstrating controllable multifunctionalities.[47] The development of SAzymes with dual-atomic sites has become a promising avenue to enhance their enzyme-like performances and further understand the fundamentals of enzyme-like reaction mechanisms.

The research on nanozymes has rapidly grown in a relatively short timeline (Fig. 1), and it is an appropriate moment to summarize the intriguing new developments in nanozyme design. This mini-review aims to capture the emerging directions in the structural evolution of nanozymes and present a full-scale picture of the nanozymes constructed with dual-atomic sites. We will start by presenting a comprehensive and systematic summary of the recent advances made in synthetic approaches and characterization methods of DACs. Then, we will discuss the current status of DAC-based nanozymes in detail highlighting representative examples. We will also show the current challenges and perspectives of DACs in nanozyme fields. It is anticipated that this review will spark more inspiring work on nanozymes and attract more attention from researchers of various backgrounds.

2. Preparation and characterization methods of DACs

The precise synthesis of DACs involves similar procedures and principles to those for SACs to a certain extent. Determining how to achieve the atomic-level dispersion and overcome the strong surface free energy without forming thermodynamically unstable phases is of great importance. The task of obtaining ideal DACs becomes even more challenging when building two metal atoms in a desired configuration is attempted. For the synthesis of both hetero- and homo-nuclear DACs, the effective manipulation of dual-atomic sites in adjacent or bridged configurations has been proved in some facile synthetic approaches, including atomic layer deposition (ALD), electrochemical deposition (ECD), chemical vapor deposition (CVD) wet chemical methods, and pyrolysis of targeted precursors (Fig. 2).[48,49] In many cases, however, some side products such as single atoms and even clusters are inevitably formed in the entire framework, which complicates the evaluation of the catalytic mechanism and the performance of DACs. Thus, it is of crucial importance to employ modern characterization techniques to confirm the precise atomic structure of the engineered DACs, too.

2.1. Strategies for constructing DACs

Isolated dual-atomic sites in DACs possess high surface energy, leading to challenges in achieving precise control over

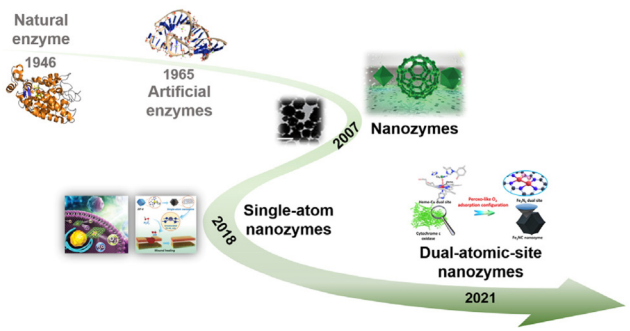

Fig. 1 Timeline of nanozyme development. Natural and artificial enzymes are shown for comparison. Reproduced with permission from ref. 1 Copyright 2007, Springer Nature; ref. 7 Copyright 2019, Royal Society of Chemistry; ref. 26 Copyright 2019, Royal Society of Chemistry; ref. 30 Copyright 2019, Wiley-VCH; ref. 88 Copyright 2019, Springer Nature.

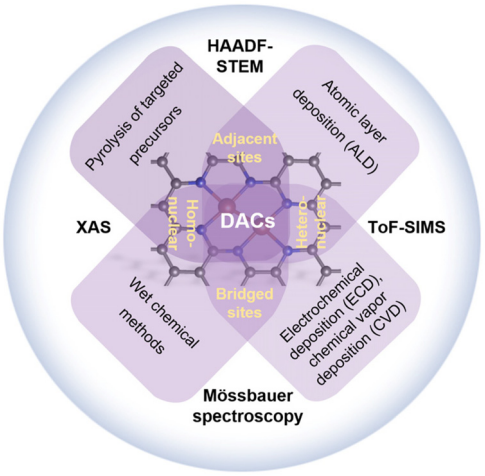

Fig. 2 Illustration of the preparation and characterization methods of DACs. HAADF-STEM: high-angle annular dark-field scanning transmission electron microscopy; XAS: X-ray absorption spectroscopy; ToF-SIMS: time-of-flight secondary ion mass spectrometry.

the synthesis of metal dimers. In this regard, the adoption of atomic layer deposition (ALD), involving a sequence of self-limiting reactions, can serve as a powerful approach for fabricating DACs with a uniform deposition character. Lu's group reported a precise bottom-up synthesis for Pt_2 dimers in a sequential manner using the ALD technique (Fig. 3a).[50] A secondary Pt atom was selectively deposited on the preliminary Pt_1 single-atom sites through the creation of proper nucleation sites in two ALD cycles. The self-limiting nature of ALD combined with orientated surface nucleation sites successfully achieved the synthesis of Pt_2 dimers with a high surface area. The ALD method was also extended to heteronuclear DACs. As demonstrated in Fig. 3b, the isolated Pt atoms were first anchored on the surface of N-doped carbon nanotubes under the optimized ALD deposition conditions.[51] By the ALD of Ru precursors on Pt single atoms under precise control, Pt–Ru dimers were successfully constructed. However, the large-scale production of DACs by the ALD technique is challenging due to the special requirement for metal precursor species and expensive equipment. In contrast, electrochemical deposition (ECD) and chemical vapor deposition (CVD) provide more flexible compatibility for expanding the selectable ranges of metal precursors and substrates for preparing DACs.[52–54]

Another promising bottom-up strategy for fabricating DACs is the wet-chemistry method. Wet chemistry methods are some of the most widely used techniques for constructing DACs, offering a facile and straightforward approach that can be conducted in conventional chemistry laboratories, without the necessity for specialized techniques or costly equipment. This method leverages dinuclear metal complexes as pre-determined precursors, providing substantial potential for the precise construction of the targeted dual-atomic configurations. Various viable approaches, including co-precipitation procedures, solvothermal/hydrothermal reactions, and (electro)chemical reduction processes, are employed to introduce these dual-atom precursors into both organic and inorganic substrates. Notably, Wang and co-workers proposed a "precursor-preselected" wet-chemistry strategy for the synthesis of mesoporous carbon nitride-supported Fe_2 cluster catalysts (Fe_2/mpg-C_3N_4).[55] This method capitalizes on preselected metal precursors to ensure the formation of specific diatomic Fe clusters, rich in anchoring sites and adept stabilization of mpg-C_3N_4 supports. This strategy was subsequently extended for the synthesis of dual-atom Pt_2 catalysts (Pt_2/mpg-C_3N_4).[56] A diatomic Pt precursor, (ethylenediamine)iodoplatinum(II) dimer dinitrate, was anchored on the mpg-C_3N_4 substrates. More recently, this group further engaged an anion replacement deposition–precipitation (ARDP) method in the preparation of a Pd_2 dual-atomic catalyst (Pd_2 DACs, Fig. 3c).[57] The obtained Pd_2 DAC exhibited a PdN_2O_2 coordination structure akin to its precursor configuration. Noteworthy progress has also been made in introducing single Pd atoms, Pd_2 dimers, and Pd_3 trimers into the hetero-macrocycles of carbon nitride (C_3N_4) *via* microwave-assisted deposition, fine-tuning the metal precursor for precise control (Fig. 3d).[58] Furthermore, the wet-chemical approach has been expanded to include more accessible synthetic routes, enabling precise control through tunable kinetic and thermodynamic parameters. Liu's group employed a strategy of electrostatically driven self-assembly assisted by phenanthroline (Phen) ligands to fabricate La, Ni bimetallic coordination structures within conjugated boronate-ester-linked covalent organic framework (COFs) substrates.[59] This work serves as a typical example of the scalable synthesis of well-defined ligand-assisted bimetallic centers.

In addition to traditional carbon-based substrates, metal oxides can also be used for stabilizing heteronuclear DACs. Huang and co-workers pioneered this avenue by first fabricating a bimetallic carbonyl cluster as organometallic precursors.[60] The subsequent steps involved the anchoring of well-dispersed Ir single atoms (Ir_1) and Mo single atoms (Mo_1) onto TiO_2 supports (Ir_1Mo_1/TiO_2) through adsorption and pyrolysis treatments. Similarly, Su and co-workers synthesized highly active and stable single-atom Sn–Zn pairs within a CuO catalyst *via* a facile hydrothermal treatment followed by wet impregnation.[61] Soon after, Wang *et al.* employed a photochemical method to create Ir dinuclear heterogeneous catalysts (Ir DHCs). The resulting Ir DHCs catalyst features two active metal centers (Ir–O–Ir) anchored on α-Fe_2O_3 supports.[62]

Typically, the wet chemistry approach was also employed to fabricate specific precursors containing two target metal atoms, which could be subsequently treated under optimized conditions to yield DACs of highly dispersed active sites. For instance, the pyrolysis of these targeted precursors is one of

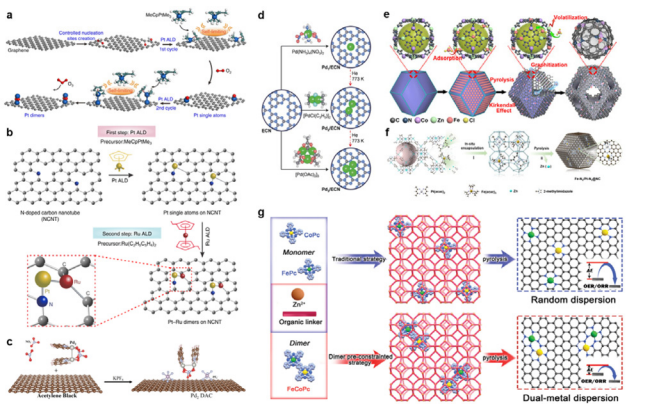

Fig. 3 Schematic diagrams illustrating the synthetic procedure of (a) dimeric Pt_2/graphene (reproduced with permission from ref. 50 Copyright 2017, Springer Nature), (b) Pt–Ru dimers on nitrogen-doped carbon nanotubes (NCNT) (reproduced with permission from ref. 51 Copyright 2019, Springer Nature), (c) supported Pd_2 DAC (reproduced with permission from ref. 57 Copyright 2021, Wiley-VCH), (d) low-nuclearity Pd catalysts (reproduced with permission from ref. 58 Copyright 2019, Wiley-VCH), (e) hollow carbon-derived nanostructures with porphyrin-like Fe–Co dual sites ((Fe,Co)/N–C) (reproduced with permission from ref. 63 Copyright 2017, American Chemical Society), (f) dual-atom Fe–N_4/Pt–N_4 sites anchored on the nitrogen-doped carbon matrix (Fe–N_4/Pt–N_4@NC) (reproduced with permission from ref. 65 Copyright 2021, Wiley-VCH), and (g) DACs based on the traditional method and the "pre-constrained metal twins" strategy (reproduced with permission from ref. 66 Copyright 2021, Wiley-VCH).

the most common synthetic methods for producing DACs. Metal–organic frameworks (MOFs), in which different metal nodes can be coordinated with multifunctional organic linkers, are of particular interest as precursors for this strategy. Moreover, the well-defined porous structures of MOFs can also endow the impregnated precursors with an ideal confinement effect at the molecular level. In an early work reported by Wu *et al.*,[63] the host–guest strategy was used to build Fe–Co dual sites embedded in nitrogen-doped carbon supports ((Fe,Co)/N–C) (Fig. 3e). A Zn/Co bimetallic MOF (BMOF) was used to host $FeCl_3$ molecules as a guest in the confined space between Zn and Co metallic nodes. A pyrolytic treatment that decomposed and graphitized the $FeCl_3$-adsorped BMOF successfully removed the vaporized Zn species and produced (Fe,Co)/N–C. Similarly, Hu *et al.* synthesized atomically dispersed binary Co–Ni sites that were anchored on N-doped hollow carbon supports (CoNi–SAs/NC) *via* a three-step synthetic strategy.[64] They first fabricated CoNi–MOFs covered with self-polymerized dopamine by chemical precipitation. The subsequent annealing under an NH_3 atmosphere and acid-leaching treatment yielded CoNi–SAs/NC. More recently, Wang and co-workers reported an *in situ* co-encapsulation method to obtain a more uniform distribution of the Fe–N_4 moiety near the adjacent Pt–N_4 moiety (Fig. 3f).[65] The sizes of two precursors, $Pt(acac)_2$ (d = ~10.0 Å) and $Fe(acac)_3$ (d = ~9.7 Å), were comparable to those of the nanocavities in zeolite imidazole frameworks-8 (ZIF-8, 11.6 Å), which ensured the uniform distribution of isolated Fe and Pt atomic sites in Fe–N_4/Pt–N_4@NC.

Since the sources of metallic sites in DACs are the metal nodes in MOF hosts or guest precursors embedded in MOFs, it is also possible to produce single-atomic and polymetallic species during the pyrolytic process due to random dispersions. Aiming to minimize such random interactions of metal species, Bu *et al.* recently reported a "pre-constrained metal twins" strategy for fabricating adjacent Fe–N_4 and Co–N_4 DACs embedded in an N-doped graphitic carbon (FeCo–DACs/NC, Fig. 3g).[66] Different from the conventional method, they first fabricated an FeCo binuclear phthalocyanine dimer and *in situ* encapsulated it into a ZIF-8 framework. After carbonization without acid treatment, FeCo–DACs/NC containing uniformly dispersed dual-metal centers were obtained. Furthermore, Niu *et al.* developed a macrocyclic precursor-mediated method to fabricate a series of DACs ranging from homonuclear to heteronuclear bimetal centers (M_1M_2–DAC).[67] The time-of-flight secondary ion mass spectrometry (ToF–SIMS) provided more definitive evidence for the formation of diatomic fragments in FeCu–DACs, while no typical signals were found in the Fe/Cu–DACs prepared by conventional co-impregnated-pyrolysis. These pioneering studies on pyrolytic methods have opened up a feasible route for constructing DACs with operational flexibility and scale–up possibility.

2.2. Characterization methods for DACs

Despite the extensive reports on the successful synthesis of DACs, some lack direct evidence for the geometric and electronic configuration of DACs due to the limitations of the characterization techniques used. The two most common characterization techniques for DACs are AC HAADF-STEM and XAS, which provide precise information about morphology and local coordination, respectively. Other spectroscopic techniques such as Mössbauer spectroscopy, electron spin resonance (ESR) spectroscopy, Fourier transform infrared (FT-IR) spectroscopy, X-ray photoelectron spectroscopy (XPS), and ultraviolet photoelectron spectroscopy (UPS) can provide complementary identification of DACs.[68]

The dimer structure of DACs was first reported by Jamie H. Warner and co-workers in 2014.[44] They directly captured the atomic structure of Fe atom pairs incorporated within a graphene lattice using an aberration-corrected transmission electron microscope (AC-TEM, Fig. 4a). Various stable structures of Fe dimers were further confirmed by the corresponding multi-slice image simulations using the atomic models based on density-functional theory (DFT) calculations (Fig. 4b and c). In general, AC HAADF-STEM presents a 2D projection along the direction of the incident beam, and thus the subtle features of dual-atomic pairs can be influenced by different projection angles. Wang's group built the spatial models of a homonuclear Fe–Fe catalyst (Fe_2–N–C), which were mainly based on the 2D projection along the direction of the incident beam (Fig. 4d).[69] The corresponding three-dimen-

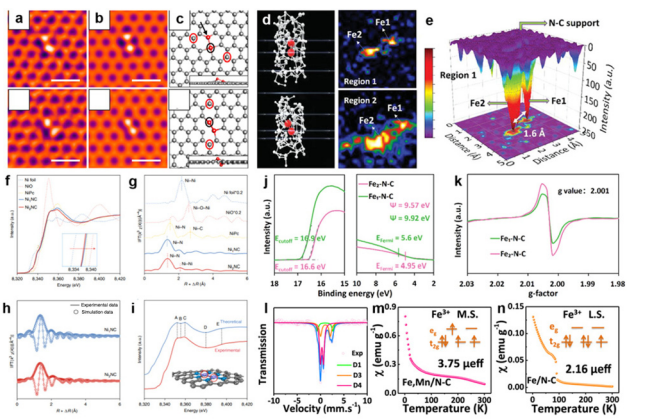

Fig. 4 (a) Smoothed aberration-corrected transmission electron microscope (AC-TEM) images, (b) multi-slice image simulations, and (c) the corresponding DFT optimized atomic models of Fe dimers in graphene vacancies. Reproduced with permission from ref. 44 Copyright 2014, American Chemical Society. (d) 2D projection along the direction of the incident beam of 3D structures and (e) 3D intensity mapping of the homonuclear Fe–Fe catalyst (Fe_2–N–C). Reproduced with permission from ref. 69 Copyright 2023, Wiley-VCH. (f) X-ray adsorption near-edge structure (XANES) spectra at the Ni K edge, (g) k^3-weighted Fourier transformed extended X-ray absorption fine structure (FT-EXAFS) spectra of Ni single-atom sites (Ni_1NC) and dual-atom sites (Ni_2NC). The corresponding fitted (h) FT-EXAFS and (i) XANES data of Ni_1NC and Ni_2NC. Reproduced with permission from ref. 76 Copyright 2022, Springer Nature. (j) UPS and (k) ESR spectra of Fe_1–N–C and Fe_2–N–C. (l) Room-temperature ^{57}Fe Mössbauer spectra and magnetic susceptibility of atomically dispersed Fe,Mn/N–C catalysts. Magnetic susceptibility of (m) Fe,Mn/N–C and (n) Fe/N–C catalysts (M.S.: medium-spin; L.S.: low-spin). Reproduced with permission from ref. 85 Copyright 2021, Springer Nature.

sional (3D) intensity map confirmed the distance of Fe–Fe atom pairs (1.6 Å, Fig. 4e). To gain comprehensive information on the atomic arrangement of DACs, more decisive tools and analysis beyond the AC HAADF-STEM are desired. For instance, electron energy loss spectroscopy (EELS) can provide high-resolution elemental mapping images that can distinguish dual-atomic species. Han and co-workers employed an EELS diagram to demonstrate the co-existence of Ni and Cu atoms in a DAC, demonstrating it to be a powerful tool for differentiating between two atoms of similar atomic numbers.[70] More recently, scanning tunneling microscopy (STM) and atom probe tomography (APT)[71–73] have been shown as important complementary characterization methods for distinguishing dimer adatoms and providing 3D constructions of DACs.

XAS is another key characterization technique to determine the electronic and geometric structure of DACs.[74,75] More specifically, X-ray absorption near-edge structure (XANES) spectroscopy can resolve electronic structures of DACs on the atomic scale. In the work by Zhang and co-workers, the absorption edge position of Ni K-edge XANES spectra was used to study the Ni electronic state in a Ni DAC (Ni_2NC),[76] and a lower Ni oxidation state in the Ni_2NC samples than that in Ni_1NC was revealed (Fig. 4f). The information on the coordinate environment of Ni sites in Ni_2NC was further analyzed using the extended X-ray absorption fine structure (EXAFS) technique that revealed two distinctive peaks at ~1.44 and 2.09 Å for the Ni–N and Ni–Ni shell, respectively (Fig. 4g). The complete local coordination structure of Ni_2NC was further refined as N_3–Ni–Ni–N_3 (Ni_2N_6) from the fitted Fourier transform-EXAFS measurements at *R* space (Fig. 4h). The simulated XANES spectrum based on a DFT model could be used to confirm the experimental data of the Ni_2N_6 configuration (Fig. 4i). In another study, Guo *et al.* used XAS to characterize the formation of Pt–Fe atomic bonds and fast electron transfer from Fe to Pt.[77] Besides these homonuclear and heteronuclear catalysts containing adjacent dual-atom sites, the bridged sites in the DACs can also be probed using XAS techniques. Zhuang *et al.* confirmed N-bridged Co–N–Ni bimetallic sites based on a series of soft and hard XAS analyses.[78] Hou and co-workers also identified an O-bridged In–Ni atomic pair in the InNi DACs using EXAFS fitting analysis.[79] It is worth noting that the XAS characterizations provide only average information regarding the entire structure of DACs. Therefore, other tools are needed to gain a more complete structural view of DACs.

Conventional XPS and UPS characterization studies offer information about the elemental composition, oxidation state, and electronic properties near the catalyst surface. The UPS spectra shown in Fig. 4j compare the surface work function (ψ) values of Fe_2–N–C and Fe_1–N–C, which have a decreased value in Fe_2–N–C due to its excellent electron-donating capability.[69] *In situ* XPS under a synchrotron light source can provide insights into the charge transfer states in DACs during operation.[80] Meanwhile, *in situ*/*operando* IR spectroscopy and Raman spectroscopy can capture the key intermediates on the DACs.[46] Electron paramagnetic resonance (EPR) is another highly sensitive spectroscopic method, particularly for the electronic structure investigation of paramagnetic species.[81,82] The enhanced EPR signal at g = 2.001 confirms a higher concentration of unpaired electrons in Fe_2–N–C than in Fe_1–N–C (Fig. 4k).

Mössbauer spectroscopy is a powerful tool for distinguishing variations in the coordination environments, local oxidation state, and spin states of Fe–, Co–, and Sn–containing catalysts.[83,84] Zhang's group employed Mössbauer spectroscopy to discriminate different Fe species in the atomically dispersed dual-metal Fe,Mn/N–C electrocatalyst (Fig. 4l).[85] The quantitative analysis confirmed that the Fe species in Fe,Mn/N–C was predominantly Fe^{III} with a medium-spin structure. For verification of the electron spin configuration, the temperature-dependent magnetic susceptibilities of Fe,Mn/N–C and Fe/N–C were compared (Fig. 4m and n). The Fe,Mn/N–C displayed a higher magnetic moment value of $3.75\mu_{eff}$ than the Fe/N–C ($2.16\mu_{eff}$) because of the greater number of unpaired *d* electrons in the medium-spin state. Besides, inductively coupled plasma mass spectrometry (ICP-MS),[86] ToF-SIMS,[67] and nuclear magnetic resonance (NMR) spectroscopy are useful characterization techniques for elucidating the structure of DACs.[87]

3. Practical applications of DACs in nanozymes

The research of employing DACs as nanozymes is still in its infancy, but its emergence itself is a key stepping stone for the development of nanozyme research. Recently, impressive progress in developing DACs with extraordinary enzyme-like behavior has been made. In the following sections, we will mainly focus on the rational design of DACs with different types of enzyme-like catalytic performance, mechanism understanding, and various biological applications.

In 2022, Zhu *et al.* designed an Fe_2NC nanozyme with an Fe–Fe dimer similar to natural cytochrome c oxidase (Fig. 5a).[88] This as-developed Fe_2NC catalyst exhibited much higher oxidase- (OXD, cytochrome c oxidase, NADH oxidase, and ascorbic acid oxidase) and peroxidase (POD, NADH peroxidase, and ascorbic acid peroxidase)-like activities compared with Fe_1NC counterparts. Liu's group further developed a multi-enzyme cascade antioxidant system by introducing Fe_2NC catalysts into Se-containing MOFs (Fe_2NC@Se, Fig. 5b).[89] The synergistic effect of Fe_2NC and Se significantly promoted the superoxide dismutase (SOD)-, catalase (CAT)-, and OXD-like performances of the Fe_2NC@Se nanozyme.

Considerable research effort has also been directed toward the exploration of heteronuclear DACs with enzyme-like performances. For instance, Zheng *et al.* successfully fabricated an atomically dispersed Fe, Pt dinuclear nanozyme, featuring Fe–N_3 and Pt–N_4 moieties (Fig. 5c).[90] This nanozyme exhibited a synergistic interplay between Fe–N_3 and Pt–N_4 sites, effectively catalyzing Fenton-like reactions and demonstrating robust photothermal conversion properties suitable for tumor

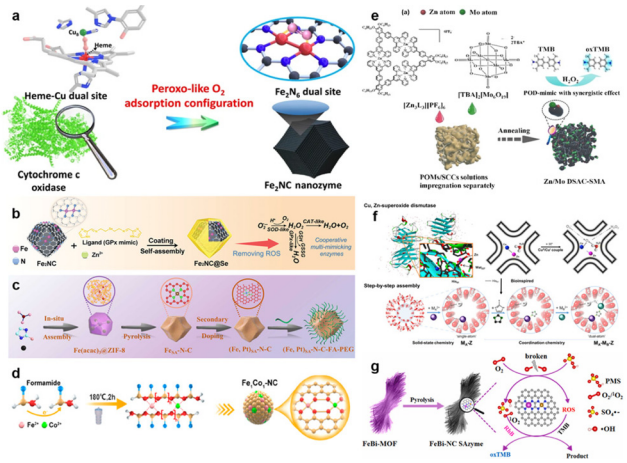

Fig. 5 (a) Schematic illustration of *peroxo*-like O_2 adsorption configuration of the Fe_2NC nanozyme. (b) The preparation process of the dual-Fe-atom nanozyme in a Se-containing MOF (Fe_2NC@Se) with multi-enzyme cascade antioxidant application. Reproduced with permission from ref. 89 Copyright 2022, Wiley-VCH. (c) Atomically dispersed Fe, Pt dinuclear catalysts ($(Fe,Pt)_{SA}$–N–C) for tumor catalytic therapy. Reproduced with permission from ref. 90 Copyright 2022, American Chemical Society. (d) Schematic illustration of the fabrication process of Fe_1Co_1–NC dual-atom metal–nitrogen–carbon nanozymes. Reproduced with permission from ref. 91 Copyright 2023, American Chemical Society. (e) Schematic illustration of the synthesis of Zn/Mo dual single atom nanozymes supported on a poly(vinyl alcohol) (PVA)-based aerogel. Reproduced with permission from ref. 92 Copyright 2022, Wiley-VCH. (f) Schematic diagrams of bio-inspired "step-by-step" assembly approach for the Zn_A–Cu_B samples as native Cu,Zn-containing superoxide dismutase (Cu,Zn–SOD) mimics. Reproduced with permission from ref. 94 Copyright 2022, Elsevier. (g) The synthesis process of Fe–Bi bimetallic MOF-derived carbon supported Fe–N_4 and Bi–N_4 dual-site FeBi–NC SAzyme. Reproduced with permission from ref. 95 Copyright 2022, Elsevier.

catalytic therapy. Song *et al.* also reported a general strategy for the development of a library of SAzymes (M_1–NC) and DAzymes (M_1/M_2–NC) with similar structures (M = Fe, Co, Ni, Mn, Ru, and Cu) (Fig. 5d).[91] The Fe_1Co_1–NC dual-atom nanozyme with Fe_1–N_4/Co_1–N_4 coordination exhibited remarkable enhancement of POD-like catalytic properties and excellent photothermal conversion efficiency. Wei's group presented a facile approach for crafting Zn/Mo dual atomic-based SAzymes (Zn/Mo DSAC–SMA) *via* the assembly of supramolecular coordination complexes and polyoxometalates (Fig. 5e).[92] The strong affinity of Mo atoms toward hydroxyl species and their subsequent migration to adjacent Zn sites, facilitated by a low energy barrier of the adsorbed hydroxyl species, resulted in a synergistic effect that substantially enhanced the H_2O_2 dissociation and POD-like performance of Zn/Mo DSAC–SMA. A Zn–Y dual-atomic catalyst having a ZnY–N_6 configuration (ZnY–DACs/NC) was also developed by Chen's group and showed POD-like performances.[93] Inspired by natural enzyme configurations, Lo's group proposed a creative approach for building dual-atom Zn_A–Cu_B bimetallic catalysts (Zn_A–Cu_B–Z) through bio-inspired synthesis procedures (Fig. 5f).[94] The structural resemblance between the synthesized Zn_A–Cu_B–Z catalysts and natural enzymes (Cu and Zn-containing SODs) makes them appealing SOD mimics. Huang *et al.* built an FeBi–NC SAzyme featuring Fe–N_4 and Bi–N_4 dual-sites within a cascade enzyme–nanozyme system for excellent peroxymonosulfate activation (Fig. 5g).[95] Furthermore, Chen's research team designed an FeCoZn catalyst containing triple-atom sites coordinated with S and N on the carbon matrix, denoted as FeCoZn–TAC/SNC. Notably, the unique architecture of FeCoZn–TAC/SNC exhibited remarkably enhanced OXD-like catalytic performance compared with those of single/dual-atom site catalysts. This distinctive design imparts great potential to FeCoZn–TAC/SNC nanozymes for the colorimetric sensing of ascorbic acid.[96]

Dual-atomic-site catalysts have demonstrated promising capabilities in emulating the multi-enzyme-like functions observed in natural enzymatic systems. This section aims to comprehend the underlying enzyme-like catalytic mechanisms inherent to dual-atomic-site SAzymes, thereby facilitating the development of next-generation SAzyme designs. Encouraged by theoretical studies based on density functional theory (DFT) calculations, Zhu's group demonstrated that the *peroxo*-like O_2 adsorption in Fe_2NC nanozymes facilitated the activation of O–O bonds with an excellent enzyme-like performance (Fig. 6a). In particular, the corresponding free-energy profiles unveiled that the adsorbed O_2 species (O_2*) tended to evolve

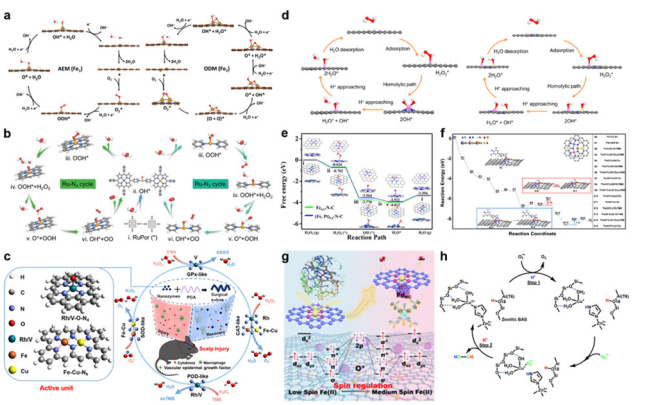

Fig. 6 (a) Schematics of the OXD-like pathway on Fe_1NC and Fe_2NC SAzymes following the adsorption evolution mechanism (AEM, left) and oxygen dissociation mechanism (ODM, right). (b) Proposed CAT-like ROS elimination pathways on Ru–N_2 and Ru–N_4 catalytic structures. Reproduced with permission from ref. 97 Copyright 2023 Wiley-VCH. (c) Single- and dual-atom nanozymes (RhN_4, VN_4, and Fe–Cu–N_6) with superior catalytic activities to accelerate scalp healing from brain trauma. Reproduced with permission from ref. 98 Copyright 2022, Springer Nature. Free energy diagrams for (d) the POD-like reaction on the Fe_1–NC and Fe_1Co_1–NC models and (e) the Fenton-like reaction mechanisms of (Fe, Pt)$_{SA}$–N–C and Fe_{SA}–N–C. (f) OXD-like energy evolution (eV) along the reaction coordinate of FeCoZn–TAC/SNC. Reproduced with permission from ref. 96 Copyright 2022, American Chemical Society. (g) Proposed reaction mechanism for engineering the spin state of Fe single-atom peroxidase-like nanozyme (FeNC) with Pd nanoclusters (PdNC). Reproduced with permission from ref. 99 Copyright 2022, Royal Society of Chemistry. (h) Proposed SOD-like reaction mechanism over Zn_A–Cu_B–Z of the zeolitic micropore.

into OOH*, O*, and OH* intermediates *via* the adsorption evolution mechanism (AEM) on the Fe_1NC OXD-like nanozyme. In contrast, Fe_2NC SAzymes showed a preference for direct O_2* dissociation, rather than forming OOH* intermediates, following the oxygen dissociation mechanism (ODM). In a parallel pursuit, Han and co-workers constructed a homogenous Ru–N_4/Ru–N_2-based dual-atomic-site SAzyme, endowed with exceptional ROS-scavenging activity (Fig. 6b).[97] They proposed and elucidated a novel nucleophilic attack pathway operating in the Ru–N_4/Ru–N_2-based CAT-like SAzymes.

Beyond the previously discussed homogenous dual-atom sites of SAzymes, Zhang and colleagues recently discovered SAzymes of RhN_4, VN_4, and Fe–Cu–N_6 configurations, each demonstrating efficient multienzyme-mimetic activities (Fig. 6c).[98] Specifically, Rh/VN_4 with an Rh/V–O–N_4 active center displayed CAT-like and glutathione peroxidase-like activities through a unique bilateral reaction mechanism, while Fe–Cu–N_6 showed impressive SOD-like activity and selectivity. Additionally, Rh/VN_4, housing Rh/V–O–N_4 active centers, displayed CAT-like and glutathione peroxidase-like activities propelled by a unique bilateral reaction mechanism. Similarly, Fe–Cu–N_6 showed impressive SOD-like activity and selectivity. A novel bilateral reaction mechanism was also proposed based on the Fe–Cu–N_6 model to explain their efficient multienzyme-mimetic catalysis. Song's group further illuminated the synergistic effect observed in Fe_1Co_1–NC dual-atom POD-like nanozymes.[91] This work revealed that the incorporation of heteronuclear metal sites induced electronic structure modulation and optimized H_2O_2 substrate adsorption (Fig. 6d). The coexistence of Fe and Co moieties facilitated diverse intermediate stabilization, ultimately reducing the overall reaction barrier. Recent studies by Zheng's group further revealed that the $(Fe, Pt)_{SA}$–N–C dinuclear nanozyme preferred a proton-mediated H_2O_2 homolytic pathway (Fig. 6e).[90] Furthermore, Chen's group designed a triple-atom FeCoZn–TAC/SNC nanozyme, showcasing strong interaction between the three metal centers, which facilitates both O_2 and TMB intermediate adsorption and activation (Fig. 6f).[96] Expanding the scope of dual-atomic site SAzymes led to the integration of single-atom sites and clusters. For example, Zhu *et al.* developed an Fe SAzyme combined with Pd nanoclusters (Pd_{NC}) as a "modulator" (FeNC–Pd_{NC}, Fig. 6g).[99] The electron-withdrawing effect of Pd_{NC} induced the spin transition of Fe active sites in FeNC–Pd_{NC}, culminating an enhanced POD-like performance. This FeNC–Pd_{NC} POD-like mimic could be applied to construct a colorimetric immunosorbent assay for the selective detection of prostate-specific antigen targets. A recent work by Lo and his colleagues unveiled that the suitable molecular distances between Zn_A–Cu_B–Z bimetallic sites would facilitate tandem enzyme-like reactions and the overall enzyme catalytic redox cycle (Fig. 6h).[94]

SAzymes featuring atomically dispersed dual-atomic sites exhibit configurations remarkably akin to those of natural enzymes, thus holding immense potential for bridging the gap between natural enzymes and nanozymes. In this section, the recent advancements in the application of emerging dual-atomic site SAzymes, encompassing domains such as biosensing, therapy treatment, and cytoprotection, are highlighted. For instance, Wei's group has established versatile biosensing platforms employing the Zn/Mo DSAC–SMA SAzyme-based system for the precise determination of intracellular H_2O_2, glucose in serum, cholesterol, and ascorbic acid in commercial beverages (Fig. 7a)[92] In a similar vein, Chen *et al.* fabricated ZnCoFe three-atom nanozymes (TAzyme) endowed with POD-like catalytic activities, which were further developed as a nanozyme sensor array for the colorimetric discrimination of phenolic acids (Fig. 7b).[100] Jin and co-workers also expanded the biosensing application of dual-atomic sites SAzyme, venturing into the electrochemiluminescence (ECL) field.[101] Benefiting from the synergistic effect exhibited by Fe, Co dual single-atom nanozymes (Fe, Co D–SACs), they successfully established an ultrasensitive luminol-dissolved O_2 (DO) ECL system together with the plasmon enhancement of AgNPs tailored for the detection of prostate-specific antigens (PSAs, Fig. 7c).

SAzymes with dual-atomic sites have received significant recognition for their exceptional OXD-, POD-, SOD-, and SOD-

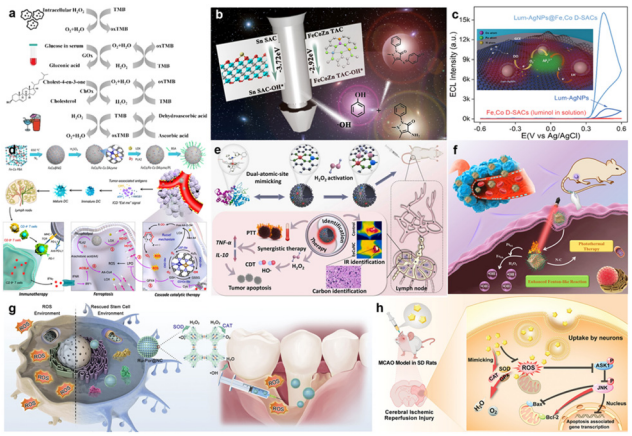

Fig. 7 Schematic illustrations of (a) a colorimetric biosensing platform for intracellular H_2O_2 detection, glucose detection in serum, cholesterol, and the ascorbic acid in commercial beverages based on the confined Zn/Mo dual single atom nanozyme, (b) visual sensor arrays for the discrimination of phenolic acids based on the ZnCoFe three-atom nanozyme, reproduced with permission from ref. 100 Copyright 2023, American Chemical Society, (c) plasmon-boosted Fe, Co dual single-atom nanozymes for constructing high-performance electrochemiluminescence (ECL) sensing platform of prostate-specific antigen targets, reproduced with permission from ref. 101 Copyright 2023, American Chemical Society, (d) FeCo/Fe–Co dual-metal atom nanozyme (FeCo/Fe–Co DAzyme) with multi-enzyme-like activities that induce cascade immunogenic ferroptosis, reproduced with permission from ref. 102 Copyright 2023, American Chemical Society, (e) biomimetic Fe–Cu dual-atomic-site nanozymes with intrinsic photothermal effect for tumor lymphatic metastasis inhibition, reproduced with permission from ref. 103 Copyright 2023, Elsevier, (f) synergistic application for tumor catalytic therapy based on $(Fe, Pt)_{SA}$–N–C dinuclear nanozymes, (g) Ru–N_4/Ru–N_2-based antioxidase-like reactive oxygen nanobiocatalysts (ROBCs) to secure stem cells and periodontal tissues, and (h) Fe_2NC@Se nanozymes with multi-enzyme cascade properties for reperfusion injury in ischemic stroke.

like attributes, endowing them with the versatility required for diverse biomedical applications. Wang and colleagues successfully prepared a six-enzyme co-expressed composite nanoplatform (FeCo/Fe–Co DAzyme/PL, Fig. 7d).[102] Leveraging the multi-enzyme-like properties of FeCo/Fe–Co DAzyme/PL, this platform could achieve immunogenic tumor ferroptosis by initiating interferon γ (IFN-γ) activation and targeting arachidonic acid (AA) metabolism. In parallel, Zhu *et al.* unveiled a biomimetic Fe–Cu dual-atomic-site SAzyme (FeCuNC), designed for efficient activation of H_2O_2 (Fig. 7e).[103] The intrinsic chemodynamic and photothermal therapies facilitated by FeCuNC SAzymes synergistically induced apoptosis in cancer cells and restrained tumor growth. Similarly, Zheng and colleagues constructed an $(Fe, Pt)_{SA}$–N–C dinuclear nanozyme, boasting a high photothermal conversion efficiency for efficient tumor catalytic therapy (Fig. 7f).[90] Moreover, reactive oxygen nanobiocatalysts (ROBCs) based on Ru–N_2 and Ru–N_4 sites exhibited proficient antioxidase-like traits, demonstrating their potential for catalytic ROS elimination through robust CAT-like degradation of H_2O_2 (Fig. 7g).[97] The unique ultrafast and reversible redox-centers intrinsic to these novel ROBCs offer robust protective effects on stem cells and periodontal tissues, accentuating their superior anti-ROS therapeutic capabilities. Furthermore, the synergistic effect of multifunctional antioxidant Fe_2NC@Se nanozymes was demonstrated to counteract oxidative damage and restrain neural apoptosis (Fig. 7h).[89]

4. Conclusions

SAzymes constructed with dual-atomic sites have attracted extensive attention and provided vast opportunities for developing next-generation nanozymes. In this mini-review, we have summarized the latest research advances made in applying DACs as nanozymes, including their synthesis strategies, characterization methods, and enzyme-like applications. Nevertheless, the development of DACs for nanozyme applications is still in the early stage, and more attention should be paid to some foreseeable challenges:

(1) Compared with SACs, achieving precise control and design in the synthesis of DACs remains a great challenge. Realizing further breakthroughs in preparation methods, precursor construction, and support selection holds great significance for advancing DACs in nanozyme research. On one front, the formation of non-uniform dual-atom sites and even clusters is a prevalent concern during DAC synthesis, hampering the scalable production of DACs with high metal loadings. Addressing this challenge is pivotal for achieving consistent and reproducible catalytic performance across various applications. Equally important, the coexistence of by-products in DACs can complicate the identification of real active sites in enzyme-like reactions. This intricacy underscores the need for precision in both synthesis and characterization to enable a thorough understanding of DACs' catalytic mechanisms. The pursuit of the goal "1 + 1 > 2" in DACs, where the combined performance surpasses the sum of individual contributions, remains a question demanding further investigation. Sustaining the advantages of DACs over SACs necessitates novel strategies to capitalize on the potential of dual-atom configurations. In this endeavor, traditional synthetic methods might prove insufficient. A promising path forward involves combining multiple approaches rather than relying solely on a single method. Some molecular models featuring hetero-polynuclear or iso-polynuclear coordination compounds (*e.g.*, MOFs, COFs, and hydrogen-bonded organic frameworks (HOFs)) hold the potential to offer the precise dual-atom configuration required for DACs.

(2) Direct identification of dual-atomic sites with conclusive evidence remains a challenge. Current characterization techniques for DACs primarily rely on HAADF–STEM images and XAS analysis, which may fall short in fully resolving and distinguishing the intricate coordination environment within DACs. Of even greater significance is the accurate identification of the dynamic evolution of dual-atomic sites in SAzymes, a critical aspect that is presently lacking. To address this gap, the development of *operando*/*in situ* characterization techniques holds promise. Such methods could offer real-time insights into the dynamic enzyme-like behaviour of dual-atomic active sites in SAzymes. Formulating a comprehensive structure–property relationship based on the dual-atom sites in SAzymes is a paramount pursuit. This endeavor is key to unraveling the intricacies of enzyme-like mechanisms at play. Such insights will not only enhance our understanding of catalytic behavior but also guide the rational design of next-generation SAzymes with improved and tailored properties. From the perspective of computational model methods, the integration of machine learning algorithms proves to be invaluable. These algorithms hold the potential to predict the complex relationship between the configuration and properties of SAzymes.

(3) Bridging the gap between homogeneous biological catalysis and heterogeneous enzyme-like catalysis through SAzymes with dual-atomic sites represents a pivotal question demanding a resolution to usher in the era of next-generation nanozymes. The current landscape of SAzymes with dual-atomic sites has largely been shaped by trial-and-error methods. However, the periodic table offers a wealth of unexplored possibilities for discovering potential SAzymes with dual-atomic sites. The pursuit of groundbreaking strategies, rooted in a deep understanding of the structure–performance relationship inherent to SAzymes with dual-atomic active centers, stands as a pressing need.

(4) The broad biomedical application of SAzymes with dual-atom sites hinges on understanding the intricate structure–biological effect relationship and ensuring long-term biosafety. A thorough biosafety assessment of DAC nanozymes stands as a prerequisite for their potential clinical translation. This concern is not exclusive to DAC-based nanozymes; it is a broader issue encompassing many nanomaterials. The inorganic nature of these heterogeneous nanozymes underscores the initial stage of their interaction with biomedicine. Thus,

substantial efforts are required to comprehensively assess the fundamental interactions between DACs and biological systems. It is noteworthy that biocompatibility is a central point of discussion for various nanomaterials. 2D nanomaterials, in particular, have shown promising initial results in terms of biocompatibility and biodegradability. These materials could serve as suitable substrates for anchoring single atoms or dual atoms in a way that preserves their catalytic activities while maintaining biocompatibility. The evolution of real-time detection techniques, such as optical imaging, holds immense potential in elucidating the relationship between the DAC configuration and biological effects. This advancement enables researchers to closely observe how DACs interact with biological systems, shedding light on critical aspects including immune responses, transport pathways, and cytotoxicity. Such insights are instrumental in understanding the biocompatibility and potential risks associated with DAC-based nanozymes.

(5) The ultimate objective of SAzymes with dual-atomic active sites is to propel the advancement of nanozymes. It is strongly anticipated that a wave of captivating research centered around dual-atomic SAzymes and their practical applications in biology is on the horizon. A comprehensive exploration of the physicochemical and biological attributes of these dual-atomic centers within SAzymes is essential to unlock their potential across diverse biomedical contexts. While the field of SAzymes with dual-atomic sites is still in its formative stages, it holds immense promise. It is believed that dual-atomic SAzymes will continually evolve, with new and more promising catalysts emerging to challenge and even replace natural enzymes in various applications.

Conflicts of interest

There are no conflicts to declare.

Acknowledgements

We acknowledge the support from the Innovation and Technology Commission and the Hong Kong Polytechnic University (1-ZVST). L. Y. S. Lee acknowledges the support from the Research Institute for Smart Energy of the Hong Kong Polytechnic University (Q-CDAG) and the Research Grants Council of the Hong Kong SAR (PolyU15217521). K.-Y. Wong acknowledges the support from the Patrick S. C. Poon Endowed Professorship.

References

1 L. Gao, J. Zhuang, L. Nie, J. Zhang, Y. Zhang, N. Gu, T. Wang, J. Feng, D. Yang, S. Perrett and X. Yan, *Nat. Nanotechnol.*, 2007, **2**, 577–583.
2 H. Wei, L. Gao, K. Fan, J. Liu, J. He, X. Qu, S. Dong, E. Wang and X. Yan, *Nano Today*, 2021, **40**, 101269.
3 A. Robert and B. Meunier, *ACS Nano*, 2022, **16**, 6956–6959.
4 Y. Huang, J. Ren and X. Qu, *Chem. Rev.*, 2019, **119**, 4357–4412.
5 D. Jiang, D. Ni, Z. T. Rosenkrans, P. Huang, X. Yan and W. Cai, *Chem. Soc. Rev.*, 2019, **48**, 3683–3704.
6 H. Wei and E. Wang, *Chem. Soc. Rev.*, 2013, **42**, 6060–6093.
7 J. Wu, X. Wang, Q. Wang, Z. Lou, S. Li, Y. Zhu, L. Qin and H. Wei, *Chem. Soc. Rev.*, 2019, **48**, 1004–1076.
8 Y. Sun, B. Xu, X. Pan, H. Wang, Q. Wu, S. Li, B. Jiang and H. Liu, *Coord. Chem. Rev.*, 2023, **475**, 214896.
9 Y. Chong, Q. Liu and C. Ge, *Nano Today*, 2021, **37**, 101076.
10 Y. Wang, R. Du, L. Y. S. Lee and K.-Y. Wong, *Biosens. Bioelectron.*, 2022, **216**, 114662.
11 L. Jiao, W. Xu, Y. Wu, H. Yan, W. Gu, D. Du, Y. Lin and C. Zhu, *Chem. Soc. Rev.*, 2021, **50**, 750–765.
12 X. Cai, L. Jiao, H. Yan, Y. Wu, W. Gu, D. Du, Y. Lin and C. Zhu, *Mater. Today*, 2021, **44**, 211–228.
13 Y. Huang, X. Mu, J. Wang, Y. Wang, J. Xie, R. Ying and E. Su, *J. Mater. Chem. B*, 2022, **10**, 1359–1368.
14 X. Li, L. Wang, D. Du, L. Ni, J. Pan and X. Niu, *TrAC, Trends Anal. Chem.*, 2019, **120**, 115653.
15 Z. Wang, R. Zhang, X. Yan and K. Fan, *Mater. Today*, 2020, **41**, 81–119.
16 X.-F. Yang, A. Wang, B. Qiao, J. Li, J. Liu and T. Zhang, *Acc. Chem. Res.*, 2013, **46**, 1740–1748.
17 Y. Wang, H. Su, Y. He, L. Li, S. Zhu, H. Shen, P. Xie, X. Fu, G. Zhou, C. Feng, D. Zhao, F. Xiao, X. Zhu, Y. Zeng, M. Shao, S. Chen, G. Wu, J. Zeng and C. Wang, *Chem. Rev.*, 2020, **120**, 12217–12314.
18 G. Jia, M. Sun, Y. Wang, X. Cui, B. Huang and J. C. Yu, *Adv. Funct. Mater.*, 2023, **33**, 2212051.
19 B. Chang, L. Zhang, S. Wu, Z. Sun and Z. Cheng, *Chem. Soc. Rev.*, 2022, **51**, 3688–3734.
20 D. Wang and Y. Zhao, *Chem*, 2021, **7**, 2635–2671.
21 B. Qiao, A. Wang, X. Yang, L. F. Allard, Z. Jiang, Y. Cui, J. Liu, J. Li and T. Zhang, *Nat. Chem.*, 2011, **3**, 634–641.
22 A. Wang, J. Li and T. Zhang, *Nat. Rev. Chem.*, 2018, **2**, 65–81.
23 X. Cui, W. Li, P. Ryabchuk, K. Junge and M. Beller, *Nat. Catal.*, 2018, **1**, 385–397.
24 L. Jiao, H. Yan, Y. Wu, W. Gu, C. Zhu, D. Du and Y. Lin, *Angew. Chem., Int. Ed.*, 2020, **59**, 2565–2576.
25 L. Huang, J. Chen, L. Gan, J. Wang and S. Dong, *Sci. Adv.*, 2019, **5**, eaav5490.
26 W. Ma, J. Mao, X. Yang, C. Pan, W. Chen, M. Wang, P. Yu, L. Mao and Y. Li, *Chem. Commun.*, 2019, **55**, 159–162.
27 Y. Wang, K. Qi, S. Yu, G. Jia, Z. Cheng, L. Zheng, Q. Wu, Q. Bao, Q. Wang, J. Zhao, X. Cui and W. Zheng, *Nano-Micro Lett.*, 2019, **11**, 102.
28 M. Zhou, Y. Jiang, G. Wang, W. Wu, W. Chen, P. Yu, Y. Lin, J. Mao and L. Mao, *Nat. Commun.*, 2020, **11**, 3188.
29 M. Chang, Z. Hou, M. Wang, D. Wen, C. Li, Y. Liu, Y. Zhao and J. Lin, *Angew. Chem., Int. Ed.*, 2022, **61**, e202209245.
30 B. Xu, H. Wang, W. Wang, L. Gao, S. Li, X. Pan, H. Wang, H. Yang, X. Meng, Q. Wu, L. Zheng, S. Chen, X. Shi,

K. Fan, X. Yan and H. Liu, *Angew. Chem., Int. Ed.*, 2019, **58**, 4911–4916.
31 Y. Wang, A. Cho, G. Jia, X. Cui, J. Shin, I. Nam, K.-J. Noh, B. J. Park, R. Huang and J. W. Han, *Angew. Chem., Int. Ed.*, 2023, e202300119.
32 Y. Wang, G. Jia, X. Cui, X. Zhao, Q. Zhang, L. Gu, L. Zheng, L. H. Li, Q. Wu, D. J. Singh, D. Matsumura, T. Tsuji, Y.-T. Cui, J. Zhao and W. Zheng, *Chem*, 2021, **7**, 436–449.
33 Y. Chen, P. Wang, H. Hao, J. Hong, H. Li, S. Ji, A. Li, R. Gao, J. Dong, X. Han, M. Liang, D. Wang and Y. Li, *J. Am. Chem. Soc.*, 2021, **143**, 18643–18651.
34 M. Chang, Z. Hou, M. Wang, C. Yang, R. Wang, F. Li, D. Liu, T. Peng, C. Li and J. Lin, *Angew. Chem., Int. Ed.*, 2021, **60**, 12971–12979.
35 G. Liao, L. Zhang, C. Li, S.-Y. Liu, B. Fang and H. Yang, *Matter*, 2022, **5**, 3341–3374.
36 S. Ji, B. Jiang, H. Hao, Y. Chen, J. Dong, Y. Mao, Z. Zhang, R. Gao, W. Chen, R. Zhang, Q. Liang, H. Li, S. Liu, Y. Wang, Q. Zhang, L. Gu, D. Duan, M. Liang, D. Wang, X. Yan and Y. Li, *Nat. Catal.*, 2021, **4**, 407–417.
37 H. Xiang, W. Feng and Y. Chen, *Adv. Mater.*, 2020, **32**, 1905994.
38 V. Kandathil and S. A. Patil, *Adv. Colloid Interface Sci.*, 2021, **294**, 102485.
39 Y. Wang, Z. Zhang, G. Jia, L. Zheng, J. Zhao and X. Cui, *Chem. Commun.*, 2019, **55**, 5271–5274.
40 W. Wu, L. Huang, E. Wang and S. Dong, *Chem. Sci.*, 2020, **11**, 9741–9756.
41 P. A. Williams, J. Cosme, A. Ward, H. C. Angove, D. Matak Vinković and H. Jhoti, *Nature*, 2003, **424**, 464–468.
42 I. G. Denisov, T. M. Makris, S. G. Sligar and I. Schlichting, *Chem. Rev.*, 2005, **105**, 2253–2278.
43 W. Zhang, Y. Chao, W. Zhang, J. Zhou, F. Lv, K. Wang, F. Lin, H. Luo, J. Li, M. Tong, E. Wang and S. Guo, *Adv. Mater.*, 2021, **33**, 2102576.
44 Z. He, K. He, A. W. Robertson, A. I. Kirkland, D. Kim, J. Ihm, E. Yoon, G.-D. Lee and J. H. Warner, *Nano Lett.*, 2014, **14**, 3766–3772.
45 Y. Wang, B. J. Park, V. K. Paidi, R. Huang, Y. Lee, K.-J. Noh, K.-S. Lee and J. W. Han, *ACS Energy Lett.*, 2022, **7**, 640–649.
46 G. Jia, M. Sun, Y. Wang, Y. Shi, L. Zhang, X. Cui, B. Huang and J. C. Yu, *Adv. Funct. Mater.*, 2022, **32**, 2206817.
47 R. Li and D. Wang, *Adv. Energy Mater.*, 2022, **12**, 2103564.
48 L. Li, K. Yuan and Y. Chen, *Acc. Mater. Res.*, 2022, **3**, 584–596.
49 A. Pedersen, J. Barrio, A. Li, R. Jervis, D. J. L. Brett, M. M. Titirici and I. E. L. Stephens, *Adv. Energy Mater.*, 2022, **12**, 2102715.
50 H. Yan, Y. Lin, H. Wu, W. Zhang, Z. Sun, H. Cheng, W. Liu, C. Wang, J. Li, X. Huang, T. Yao, J. Yang, S. Wei and J. Lu, *Nat. Commun.*, 2017, **8**, 1070.
51 L. Zhang, R. Si, H. Liu, N. Chen, Q. Wang, K. Adair, Z. Wang, J. Chen, Z. Song, J. Li, M. N. Banis, R. Li, T.-K. Sham, M. Gu, L.-M. Liu, G. A. Botton and X. Sun, *Nat. Commun.*, 2019, **10**, 4936.
52 L. Bai, C.-S. Hsu, D. T. L. Alexander, H. M. Chen and X. Hu, *J. Am. Chem. Soc.*, 2019, **141**, 14190–14199.
53 Z. Zhang, C. Feng, C. Liu, M. Zuo, L. Qin, X. Yan, Y. Xing, H. Li, R. Si, S. Zhou and J. Zeng, *Nat. Commun.*, 2020, **11**, 1215.
54 Y. Yang, Y. Qian, H. Li, Z. Zhang, Y. Mu, D. Do, B. Zhou, J. Dong, W. Yan, Y. Qin, L. Fang, R. Feng, J. Zhou, P. Zhang, J. Dong, G. Yu, Y. Liu, X. Zhang and X. Fan, *Sci. Adv.*, 2020, **6**, eaba6586.
55 S. Tian, Q. Fu, W. Chen, Q. Feng, Z. Chen, J. Zhang, W.-C. Cheong, R. Yu, L. Gu, J. Dong, J. Luo, C. Chen, Q. Peng, C. Draxl, D. Wang and Y. Li, *Nat. Commun.*, 2018, **9**, 2353.
56 S. Tian, B. Wang, W. Gong, Z. He, Q. Xu, W. Chen, Q. Zhang, Y. Zhu, J. Yang, Q. Fu, C. Chen, Y. Bu, L. Gu, X. Sun, H. Zhao, D. Wang and Y. Li, *Nat. Commun.*, 2021, **12**, 3181.
57 N. Zhang, X. Zhang, Y. Kang, C. Ye, R. Jin, H. Yan, R. Lin, J. Yang, Q. Xu, Y. Wang, Q. Zhang, L. Gu, L. Liu, W. Song, J. Liu, D. Wang and Y. Li, *Angew. Chem., Int. Ed.*, 2021, **60**, 13388–13393.
58 E. Vorobyeva, E. Fako, Z. Chen, S. M. Collins, D. Johnstone, P. A. Midgley, R. Hauert, O. V. Safonova, G. Vilé, N. López, S. Mitchell and J. Pérez-Ramírez, *Angew. Chem., Int. Ed.*, 2019, **58**, 8724–8729.
59 M. Zhou, Z. Wang, A. Mei, Z. Yang, W. Chen, S. Ou, S. Wang, K. Chen, P. Reiss, K. Qi, J. Ma and Y. Liu, *Nat. Commun.*, 2023, **14**, 2473.
60 J. Fu, J. Dong, R. Si, K. Sun, J. Zhang, M. Li, N. Yu, B. Zhang, M. G. Humphrey, Q. Fu and J. Huang, *ACS Catal.*, 2021, **11**, 1952–1961.
61 Q. Shi, Y. Ji, W. Chen, Y. Zhu, J. Li, H. Liu, Z. Li, S. Tian, L. Wang, Z. Zhong, L. Wang, J. Ma, Y. Li and F. Su, *Natl. Sci. Rev.*, 2019, **7**, 600–608.
62 Y. Zhao, K. R. Yang, Z. Wang, X. Yan, S. Cao, Y. Ye, Q. Dong, X. Zhang, J. E. Thorne, L. Jin, K. L. Materna, A. Trimpalis, H. Bai, S. C. Fakra, X. Zhong, P. Wang, X. Pan, J. Guo, M. Flytzani-Stephanopoulos, G. W. Brudvig, V. S. Batista and D. Wang, *Proc. Natl. Acad. Sci. U. S. A.*, 2018, **115**, 2902–2907.
63 J. Wang, Z. Huang, W. Liu, C. Chang, H. Tang, Z. Li, W. Chen, C. Jia, T. Yao, S. Wei, Y. Wu and Y. Li, *J. Am. Chem. Soc.*, 2017, **139**, 17281–17284.
64 X. Han, X. Ling, D. Yu, D. Xie, L. Li, S. Peng, C. Zhong, N. Zhao, Y. Deng and W. Hu, *Adv. Mater.*, 2019, **31**, 1905622.
65 A. Han, X. Wang, K. Tang, Z. Zhang, C. Ye, K. Kong, H. Hu, L. Zheng, P. Jiang, C. Zhao, Q. Zhang, D. Wang and Y. Li, *Angew. Chem., Int. Ed.*, 2021, **60**, 19262–19271.
66 M. Liu, N. Li, S. Cao, X. Wang, X. Lu, L. Kong, Y. Xu and X.-H. Bu, *Adv. Mater.*, 2022, **34**, 2107421.
67 Y.-X. Zhang, S. Zhang, H. Huang, X. Liu, B. Li, Y. Lee, X. Wang, Y. Bai, M. Sun, Y. Wu, S. Gong, X. Liu,

Z. Zhuang, T. Tan and Z. Niu, *J. Am. Chem. Soc.*, 2023, **145**, 4819–4827.
68 Y. Ying, X. Luo, J. Qiao and H. Huang, *Adv. Funct. Mater.*, 2021, **31**, 2007423.
69 Y. Song, F. Kong, X. Sun, Q. Liu, X. Li, L. Ren, Y. Xie, Y. Shen and J. Wang, *Adv. Energy Mater.*, 2023, **13**, 2203660.
70 L. Zhang, J. Feng, S. Liu, X. Tan, L. Wu, S. Jia, L. Xu, X. Ma, X. Song, J. Ma, X. Sun and B. Han, *Adv. Mater.*, 2023, 2209590, DOI: **10.1002/adma.202209590**.
71 F. Kraushofer, L. Haager, M. Eder, A. Rafsanjani-Abbasi, Z. Jakub, G. Franceschi, M. Riva, M. Meier, M. Schmid, U. Diebold and G. S. Parkinson, *ACS Energy Lett.*, 2022, **7**, 375–380.
72 K. Jiang, S. Back, A. J. Akey, C. Xia, Y. Hu, W. Liang, D. Schaak, E. Stavitski, J. K. Nørskov, S. Siahrostami and H. Wang, *Nat. Commun.*, 2019, **10**, 3997.
73 K. Jiang, S. Siahrostami, A. J. Akey, Y. Li, Z. Lu, J. Lattimer, Y. Hu, C. Stokes, M. Gangishetty, G. Chen, Y. Zhou, W. Hill, W.-B. Cai, D. Bell, K. Chan, J. K. Nørskov, Y. Cui and H. Wang, *Chem*, 2017, **3**, 950–960.
74 H. Fei, J. Dong, Y. Feng, C. S. Allen, C. Wan, B. Volosskiy, M. Li, Z. Zhao, Y. Wang, H. Sun, P. An, W. Chen, Z. Guo, C. Lee, D. Chen, I. Shakir, M. Liu, T. Hu, Y. Li, A. I. Kirkland, X. Duan and Y. Huang, *Nat. Catal.*, 2018, **1**, 63–72.
75 Y. Wang, X. Cui, J. Zhao, G. Jia, L. Gu, Q. Zhang, L. Meng, Z. Shi, L. Zheng, C. Wang, Z. Zhang and W. Zheng, *ACS Catal.*, 2019, **9**, 336–344.
76 Q. Hao, H.-X. Zhong, J.-Z. Wang, K.-H. Liu, J.-M. Yan, Z.-H. Ren, N. Zhou, X. Zhao, H. Zhang, D.-X. Liu, X. Liu, L.-W. Chen, J. Luo and X.-B. Zhang, *Nat. Synth.*, 2022, **1**, 719–728.
77 X. Miao, W. Chen, S. Lv, A. Li, Y. Li, Q. Zhang, Y. Yue, H. Zhao, L. Liu, S. Guo and L. Guo, *Adv. Mater.*, 2023, 2211790, DOI: **10.1002/adma.202211790**.
78 J. Pei, T. Wang, R. Sui, X. Zhang, D. Zhou, F. Qin, X. Zhao, Q. Liu, W. Yan, J. Dong, L. Zheng, A. Li, J. Mao, W. Zhu, W. Chen and Z. Zhuang, *Energy Environ. Sci.*, 2021, **14**, 3019–3028.
79 Z. Fan, R. Luo, Y. Zhang, B. Zhang, P. Zhai, Y. Zhang, C. Wang, J. Gao, W. Zhou, L. Sun and J. Hou, *Angew. Chem., Int. Ed.*, 2023, **62**, e202216326.
80 X. Li, X. Yang, J. Zhang, Y. Huang and B. Liu, *ACS Catal.*, 2019, **9**, 2521–2531.
81 S. Baumann, W. Paul, T. Choi, C. P. Lutz, A. Ardavan and A. J. Heinrich, *Science*, 2015, **350**, 417–420.
82 C. Ling, X. Liu, H. Li, X. Wang, H. Gu, K. Wei, M. Li, Y. Shi, H. Ben, G. Zhan, C. Liang, W. Shen, Y. Li, J. Zhao and L. Zhang, *Angew. Chem., Int. Ed.*, 2022, **61**, e202200670.
83 U. I. Kramm, L. Ni and S. Wagner, *Adv. Mater.*, 2019, **31**, 1805623.
84 G.-F. Han, F. Li, A. I. Rykov, Y.-K. Im, S.-Y. Yu, J.-P. Jeon, S.-J. Kim, W. Zhou, R. Ge, Z. Ao, T. J. Shin, J. Wang, H. Y. Jeong and J.-B. Baek, *Nat. Nanotechnol.*, 2022, **17**, 403–407.
85 G. Yang, J. Zhu, P. Yuan, Y. Hu, G. Qu, B.-A. Lu, X. Xue, H. Yin, W. Cheng, J. Cheng, W. Xu, J. Li, J. Hu, S. Mu and J.-N. Zhang, *Nat. Commun.*, 2021, **12**, 1734.
86 A. A. Ammann, *J. Mass Spectrom.*, 2007, **42**, 419–427.
87 G. Lalande, R. Côté, G. Tamizhmani, D. Guay, J. P. Dodelet, L. Dignard-Bailey, L. T. Weng and P. Bertrand, *Electrochim. Acta*, 1995, **40**, 2635–2646.
88 L. Jiao, W. Ye, Y. Kang, Y. Zhang, W. Xu, Y. Wu, W. Gu, W. Song, Y. Xiong and C. Zhu, *Nano Res.*, 2022, **15**, 959–964.
89 R. Tian, H. Ma, W. Ye, Y. Li, S. Wang, Z. Zhang, S. Liu, M. Zang, J. Hou, J. Xu, Q. Luo, H. Sun, F. Bai, Y. Yang and J. Liu, *Adv. Funct. Mater.*, 2022, **32**, 2204025.
90 S. Wang, Z. Hu, Q. Wei, P. Cui, H. Zhang, W. Tang, Y. Sun, H. Duan, Z. Dai, Q. Liu and X. Zheng, *ACS Appl. Mater. Interfaces*, 2022, **14**, 20669–20681.
91 R. Zeng, Y. Li, X. Hu, W. Wang, Y. Li, H. Gong, J. Xu, L. Huang, L. Lu, Y. Zhang, D. Tang and J. Song, *Nano Lett.*, 2023, **23**, 6073–6080.
92 C.-B. Ma, Y. Xu, L. Wu, Q. Wang, J.-J. Zheng, G. Ren, X. Wang, X. Gao, M. Zhou, M. Wang and H. Wei, *Angew. Chem., Int. Ed.*, 2022, **61**, e202116170.
93 X. Jin, X. Feng, G. Wang, R. Tan, Y. Peng, L. Zheng, W. Chen and Z. Chen, *J. Mater. Chem. A*, 2023, **11**, 2326–2333.
94 C. K. T. Wun, H. K. Mok, T. Chen, T.-S. Wu, K. Taniya, K. Nakagawa, S. Day, C. C. Tang, Z. Huang, H. Su, W.-Y. Yu, T. K. W. Lee and T. W. B. Lo, *Chem. Catal.*, 2022, **2**, 2346–2363.
95 Q. Chen, Y. Liu, Y. Lu, Y. Hou, X. Zhang, W. Shi and Y. Huang, *J. Hazard. Mater.*, 2022, **422**, 126929.
96 R. Wu, M. Sun, X. Liu, F. Qin, X. Zhang, Z. Qian, J. Huang, Y. Li, T. Tan, W. Chen and Z. Chen, *Anal. Chem.*, 2022, **94**, 14308–14316.
97 J. Guo, Z. Xing, L. Liu, Y. Sun, H. Zhou, M. Bai, X. Liu, M. Adeli, C. Cheng and X. Han, *Adv. Funct. Mater.*, 2023, **33**, 2211778.
98 S. Zhang, Y. Li, S. Sun, L. Liu, X. Mu, S. Liu, M. Jiao, X. Chen, K. Chen, H. Ma, T. Li, X. Liu, H. Wang, J. Zhang, J. Yang and X.-D. Zhang, *Nat. Commun.*, 2022, **13**, 4744.
99 X. Wei, S. Song, W. Song, Y. Wen, W. Xu, Y. Chen, Z. Wu, Y. Qin, L. Jiao, Y. Wu, M. Sha, J. Huang, X. Cai, L. Zheng, L. Hu, W. Gu, M. Eguchi, T. Asahi, Y. Yamauchi and C. Zhu, *Chem. Sci.*, 2022, **13**, 13574–13581.
100 J. Huang, H. Gu, G. Wang, R. Wu, M. Sun and Z. Chen, *Anal. Chem.*, 2023, **95**, 9107–9115.
101 F. A. Bushira, P. Wang, Y. Wang, S. Hou, X. Diao, H. Li, L. Zheng and Y. Jin, *Anal. Chem.*, 2022, **94**, 9758–9765.
102 Y. Liu, R. Niu, R. Deng, S. Song, Y. Wang and H. Zhang, *J. Am. Chem. Soc.*, 2023, **145**, 8965–8978.
103 L. Jiao, N. Tao, Y. Kang, W. Song, Y. Chen, Y. Zhang, W. Xu, Y. Wu, W. Gu, L. Zheng, L. Chen, L. Deng, C. Zhu and Y.-N. Liu, *Nano Today*, 2023, **50**, 101859.